applied sciences

MDPI

Article

Thermal Stability of Ionic Liquids: Effect of Metals

Francesca Nardelli [1,2], Emilia Bramanti [2], Alessandro Lavacchi [3], Silvia Pizzanelli [2,4], Beatrice Campanella [2], Claudia Forte [2,4], Enrico Berretti [3] and Angelo Freni [2,*]

[1] Dipartimento di Chimica e Chimica Industriale, Università di Pisa, Via G. Moruzzi 13, 56124 Pisa, Italy; francesca.nardelli@dcci.unipi.it
[2] Istituto di Chimica dei Composti OrganoMetallici, Consiglio Nazionale delle Ricerche, Via G. Moruzzi 1, 56124 Pisa, Italy; emilia.bramanti@pi.iccom.cnr.it (E.B.); silvia.pizzanelli@pi.iccom.cnr.it (S.P.); beatrice.campanella@pi.iccom.cnr.it (B.C.); claudia.forte@pi.iccom.cnr.it (C.F.)
[3] Istituto di Chimica dei Composti OrganoMetallici, Consiglio Nazionale delle Ricerche, Via Madonna del Piano 10, 50019 Firenze, Italy; alessandro.lavacchi@iccom.cnr.it (A.L.); enrico.berretti@iccom.cnr.it (E.B.)
[4] Centre for Instrument Sharing (CISUP), University of Pisa, Lungarno Pacinotti 43, 56126 Pisa, Italy
* Correspondence: angelo.freni@pi.iccom.cnr.it

Abstract: We investigated the thermal stability and corrosion effects of a promising ionic liquid (IL) to be employed as an advanced heat transfer fluid in solar thermal energy applications. Degradation tests were performed on IL samples kept in contact with various metals (steel, copper and brass) at 200 °C for different time lengths. Structural characterization of fresh and aged IL samples was carried out by high-resolution magic angle spinning nuclear magnetic resonance and Fourier transform infrared spectroscopic analyses, while headspace gas chromatography–mass spectrometry was employed to evaluate the release of volatile organic compounds. The combination of the above-mentioned techniques effectively allowed the occurrence of degradation processes due to aging to be verified.

Keywords: ionic liquids; heat storage; thermal stability; HRMAS NMR; FTIR

Citation: Nardelli, F.; Bramanti, E.; Lavacchi, A.; Pizzanelli, S.; Campanella, B.; Forte, C.; Berretti, E.; Freni, A. Thermal Stability of Ionic Liquids: Effect of Metals. *Appl. Sci.* **2022**, *12*, 1652. https://doi.org/10.3390/app12031652

Academic Editors: Angela Malara and Frontera Patrizia

Received: 5 January 2022
Accepted: 1 February 2022
Published: 4 February 2022

1. Introduction

Ionic liquids (ILs) are a group of compounds that are attracting increasing interest in many fields of application, thanks to the possibility of combining different anions and cations, thus allowing the design of new materials with optimal chemical–physical properties for specific applications, especially in the energy sector [1,2]. In particular, ILs are suggested as promising working fluids in solar energy technologies, thanks to their high heat capacity, low melting point and relatively high density in the typical operating conditions of solar thermal energy systems [3–6]. Further attractive features of ILs are the high chemical stability, non-flammability, and the low impact on the environment and on health; this feature derives from their negligible vapor pressure, which limits their release in the atmosphere [7]. Given the wide application potential, evaluation of ILs' thermal stability is fundamental for their implementation in solar energy systems as working fluids [8–10].

Most of the thermal stability studies available in the literature are based on dynamic thermogravimetric (TG) analyses [11,12]. However, several experimental parameters, such as sample mass, pre-treatment conditions, heating rate and testing atmosphere (inert gas or open air), can affect measurement consistency [13]; therefore, TG analysis appears to be more appropriate for comparative thermal stability studies [14], and certainly cannot provide a deep insight into the modifications of the IL structure due to thermal stress. Another issue of relevance is metal corrosion in the presence of ILs. In fact, several R&D activities in the field have focused on the investigation of the corrosion behavior of different metals in contact with ILs, and on the evaluation of the release of volatile compounds during operation in solar thermal devices and processes [15–19].

To address the previously mentioned issues, in this paper, we present a multi-technique approach to identify possible degradation products of a promising IL subjected to thermal aging in the absence or presence of different metals. Specifically, we have characterized the ionic liquid N-tributyl-N-methylammonium bis(trifluoromethanesulfonyl)imide ([TBuMA][NTF_2]) after thermal treatment at T = 200 °C for 4, 24 and 168 h in contact with AISI 304 steel, copper or brass, as well as in the absence of metals. The temperature used for aging was selected because it is the standard operating temperature of common diathermic oils used as heat transfer fluids. This specific ammonium-based IL compound was chosen for its potential application as a heat transfer fluid [5,12], and for the stability of the anion [20], which has been reported to withstand temperatures up to 400 °C by thermogravimetry. However, to the best of our knowledge, there is no indication of the thermal stability of NTF_2 coupled with a quaternary ammonium salt. The characterization of the degraded IL was carried out by high-resolution magic angle spinning nuclear magnetic resonance (HRMAS NMR) and Fourier transform infrared (FTIR) spectroscopies, while headspace gas chromatography–mass spectrometry (HS-GC-MS) was employed to estimate the concentration of volatile compounds produced. HRMAS NMR is suitable for the characterization of highly viscous liquids. In this tecnique, the use of magic angle spinning allows highly resolved spectra to be obtained, which is not feasible using standard solution NMR spectroscopy, due to the presence of residual interactions and magnetic susceptibility issues [21].

2. Materials and Methods

2.1. Materials

The ionic liquid N-tributyl-N-methylammonium bis(trifluoromethanesulfonyl)imide ($C_{15}H_{30}F_6N_2O_4S_2$), CAS number 405514-94-5; MW 480.53, Figure 1a, was purchased from Solvionic (Am3408a). Purity of the IL was 99.9%.

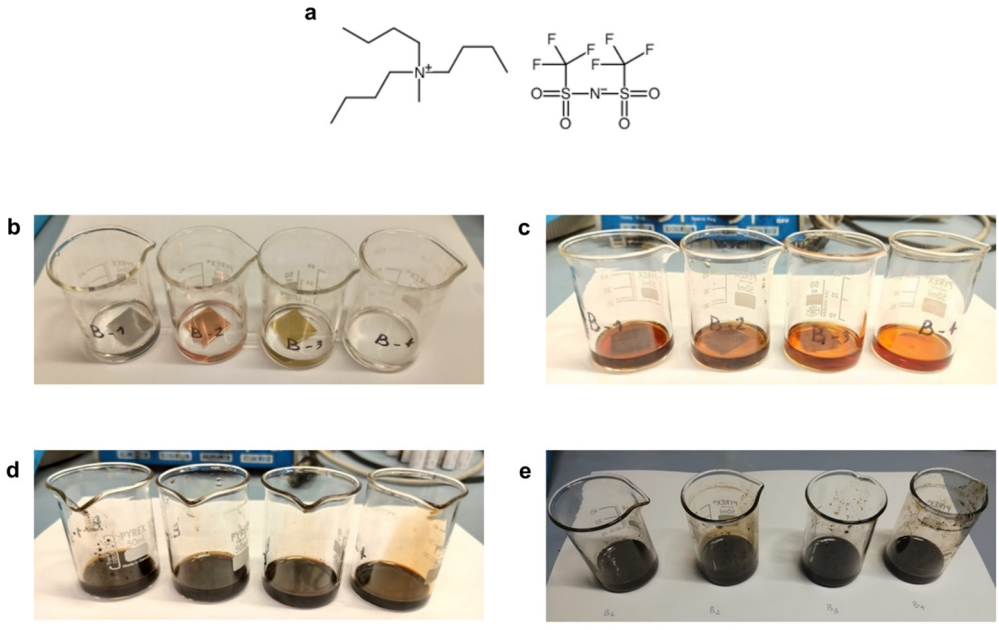

Figure 1. (**a**) Structure of the ionic liquid [TBuMA][NTF_2]. (**b**) In sequence, from left to right, samples of the ionic liquid in the presence of steel, copper and brass metal plates and with no metal plate. The same samples were heated at 200 °C for 4 h (**c**), 24 h (**d**) and 168 h (**e**).

The degradation procedure was performed as described in the following. Six milliliters of [TBuMA][NTF_2] was heated in an oven at 200 °C for 7 days with or without a steel, copper or brass metal plate (2 × 2 cm). At selected times (4, 24 and 168 h; Figure 1b–e,

respectively), 1 mL of IL was sampled for the analyses (FTIR, HS-GC-MS and HRMAS NMR spectroscopy).

Table 1 summarizes the thermally treated samples analyzed and the code used throughout the text. The code of the initial non-heated sample is B.

Table 1. Sample codes of the IL samples.

Metal	4 h at 200 °C	24 h at 200 °C	168 h at 200 °C
1 (steel)	1B4	1B24	1B168
2 (copper)	2B4	2B24	2B168
3 (brass)	3B4	3B24	3B168
4 (no metal)	4B4	4B24	4B168

2.2. FTIR Spectroscopy

Infrared spectra were recorded in reflectance mode by using a Perkin–Elmer Frontiers FTIR Spectrophotometer, equipped with a universal attenuated total reflectance (ATR) accessory and a triglycine sulphate TGS detector. Three replicates (3–5 μL of IL for each measurement) were performed after background acquisition. For each sample, 32 scans were recorded, averaged and Fourier transformed to produce a spectrum with a nominal resolution of 4 cm^{-1}.

2.3. HS-GC-MS Analysis

HS-GC-MS analyses were performed using an Agilent 6850 gas chromatograph, equipped with a split/splitless injector, in combination with an Agilent 5975c mass spectrometer. A CTC CombiPAL autosampler was employed for HS sampling. Vials with 1 g of sample were incubated at 80 °C for 15 min. A 0.5 mL HS volume was then sampled (gas-tight syringe held at 85 °C) and injected into the GC. The syringe was then flushed with helium. The inlet liner (internal diameter of 1 mm) was held at 200 °C and the injection was performed in splitless mode. Compounds were separated on a polar column (DB-WAX ultra-inert; length: 30 m; stationary phase: bonded polyethylene glycol; 0.25 mm inner diameter; 0.50 μm coating) using the following temperature program: 10 min at 30 °C, then increased by 5 °C/min to 60 °C (held for 2 min) followed by an increase of 10 °C/min to 240 °C (held for 9 min). The temperature of the transfer line was set at 250 °C. After GC separation, compounds were ionized in positive EI, and the acquisition was performed in full scan mode. Spectral identification was performed when the spectra and the NIST spectral mass library (NIST 05) combined with our in-house library matched with a spectral similarity >90%. Results are reported as relative intensity (counts).

2.4. HRMAS NMR Spectroscopy

NMR spectra were acquired on a Bruker AVANCE NEO NMR Spectrometer, working at a ^{1}H Larmor frequency of 500.13 and 125.77 MHz for ^{1}H and ^{13}C nuclei, respectively, and using an HRMAS probe. All samples were spun at 6 kHz. The samples were dissolved in DMSO-d_6 (99.7% deuterated, Sigma) (1:1 volume ratio) to provide the lock signal and to reduce their viscosity, thus facilitating their insertion in the rotors; TMS was added to each mixture for ^{1}H spectral referencing. Following this, 50 μL of each mixture was transferred to an HRMAS rotor for NMR analysis. ^{1}H spectra were acquired on all samples using a relaxation delay of 1 s and several scans ranging from 128 to 1000 depending on the sample. ^{13}C spectra were acquired on samples B, 1B168, 2B168 and 4B168 using the Bruker *zg30pg* pulse sequence for NOE enhancement of carbon nuclei signals. A relaxation delay of 2 s was used and 4k scans were accumulated. One-dimensional (1D) selective ^{1}H total correlation spectroscopy (TOCSY) and two-dimensional (2D) ^{1}H-^{13}C heteronuclear single quantum coherence (HSQC) experiments were also performed on sample 4B168. For the TOCSY experiments, the Bruker *seldigpzs* pulse sequence was used, with a Gaussian shaped 180° pulse (Bruker pulse shape: Gaus1_180r.1000) for selective excitation, a relaxation delay of 1 s, and a mixing time of 80 ms. ^{1}H–^{13}C HSQC were obtained by employing the Bruker

hsqcetgpsisp2.2 pulse sequence, with a relaxation delay of 1 s. For all experiments, a ^{1}H 90° pulse of 7 µs and a ^{13}C 90° pulse of 12 µs were used. All experiments were performed at 298 K.

3. Results and Discussion

Figure 1 shows that, after 4 h, all the samples displayed a brown color, indicating that the thermal treatment degrades [TBuMA][NTF_2]. The color was more intense in the presence of metals, particularly steel and copper, and became darker with longer heating times. To understand the decomposition pathway(s), FTIR and HRMAS NMR experiments were performed on all the samples. Figure 2 shows the ATR-FTIR spectra of [TBuMA][NTF_2] after 4, 24 and 168 h (samples 4B4, 4B24 and 4B168) of thermal treatment without metal plates. The spectrum of untreated IL (sample B) is also reported for comparison.

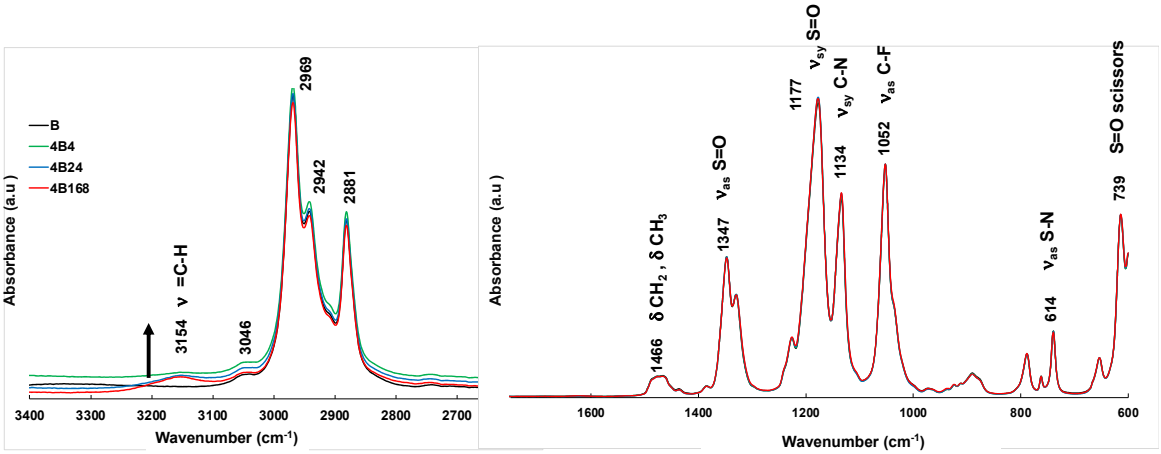

Figure 2. Representative ATR-FTIR spectra of B, 4B4, 4B24 and 4B168 samples in the 3400–2650 and 1740−600 cm^{-1} regions.

As far as the IL anion is concerned, the strong absorptions at 1347 and 1177 cm^{-1} are attributed to asymmetric and symmetric S=O stretching vibrations, respectively, the band at 1052 cm^{-1} to asymmetric C–F stretching, the band at 739 cm^{-1} to asymmetric S–N stretching, and the band at 614 cm^{-1} to S=O scissoring. Specific TBuMA cation signals are expected at 1134 cm^{-1}, ascribable to symmetric C–N stretching, around 1470 cm^{-1} due to methyl and methylene C–H bending, and at 1465 and 1378 cm^{-1} due to C–H scissoring and methyl rocking, respectively. The spectra of all the samples are basically identical, except for slight differences in the 3250–3000 cm^{-1} region (Figure 3), suggesting that the anion is not affected by the thermal treatment, and indicating a major involvement of the cation in the thermal degradation. Inspection of this region highlights that the original structure of the TBuMA cation, characterized by the large band at 3348 cm^{-1} and the shoulder at 3040 cm^{-1}, due to ammonium absorptions, is modified after thermal treatment. The most significant changes are the decrease in the band at 3348 cm^{-1} and the increase in the peak in the region between 3200 and 3100 cm^{-1}, both in the presence and absence of metals. This peak has been assigned to the medium intensity band of unsaturated hydrogen stretches (C=C–H) [22], and suggests the formation of alkenes.

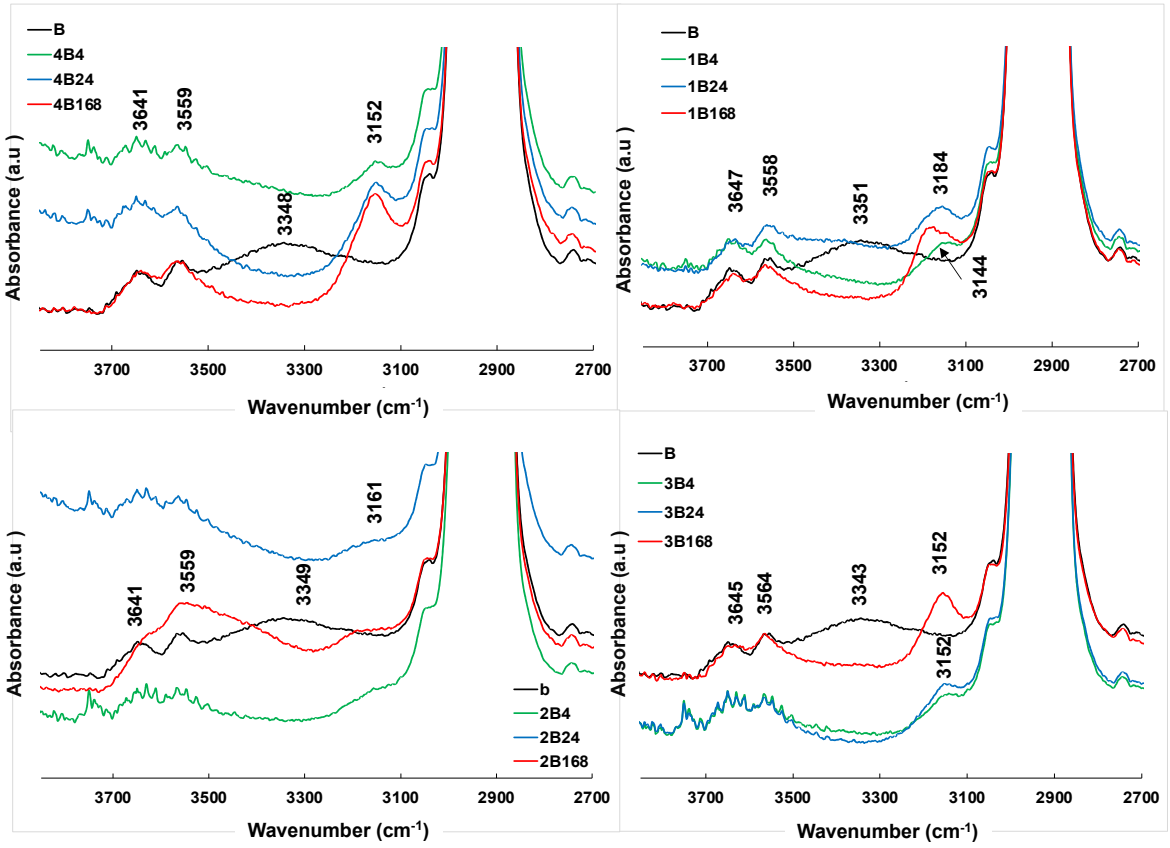

Figure 3. ATR-FTIR spectra of all samples in the 3400–2650 cm^{-1} region.

Figure 4 shows the trend of the area of the band at 3153 cm^{-1} (3208–3103 cm^{-1} baseline points) of the IL spectra with or without metal plates, as a function of the duration of the thermal treatment.

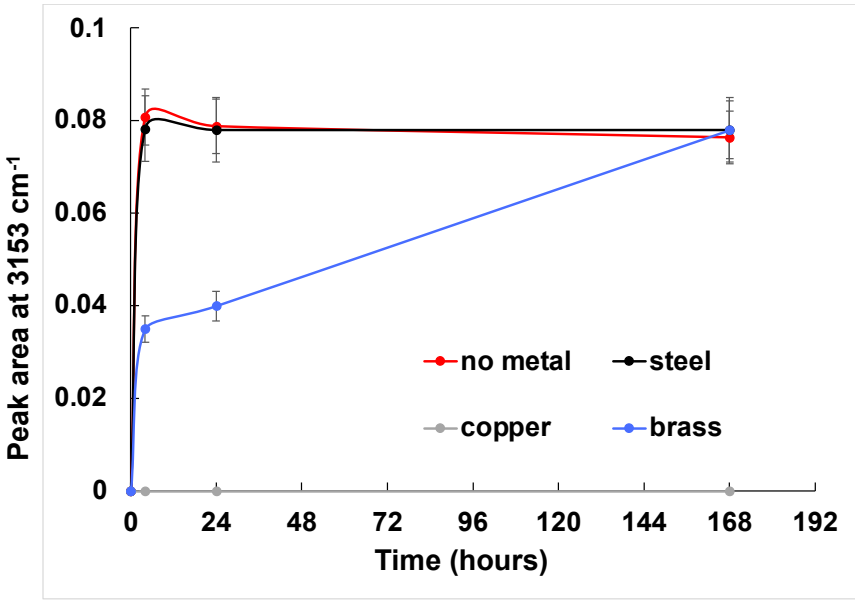

Figure 4. Area of the peak at 3153 cm^{-1} in the IL spectra after 4, 24 and 168 h of thermal treatment with or without metal plates as a function of incubation time.

Further insight on the degradation process was gained from HRMAS NMR spectroscopy. The comparison of the ^{1}H NMR spectrum of the original compound [TBuMA][NTF_2] with the spectra recorded on [TBuMA][NTF_2] after heating for 4, 24, and 168 h (samples 4B4, 4B24, and 4B168) reveals that the signals of the original cation remain dominant, even at the longest heating time. Low-intensity peaks, due to the degradation products, appear in the samples subjected to thermal treatment, and their intensity tends to increase with the heating time. Figure 5 shows the NMR spectra of samples B (traces a and b) and 4B168 (traces c and d). Four new signals, resonating at 9.16, 8.31, 2.75 and 2.57 ppm, appear in the latter. Additional signals of lower intensity appear in the region between 5 and 6 ppm upon heating. Complete characterization of the degradation compounds was accomplished by the analysis of ^{1}H, 1D selective ^{1}H TOCSY, ^{13}C and 2D ^{1}H–^{13}C HSQC spectra of 4B168 (Figures S1 and S2). The assignments of ^{1}H and ^{13}C NMR signals are reported in Tables S1 and S2.

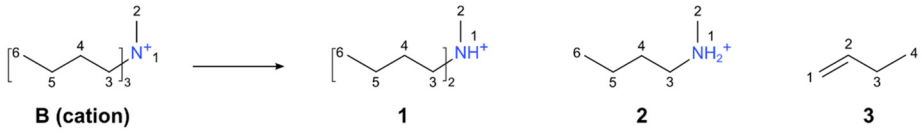

Scheme 1. Decomposition pathways of cation TBuMA. The labeling on each compound is used for the assignment of the NMR signals.

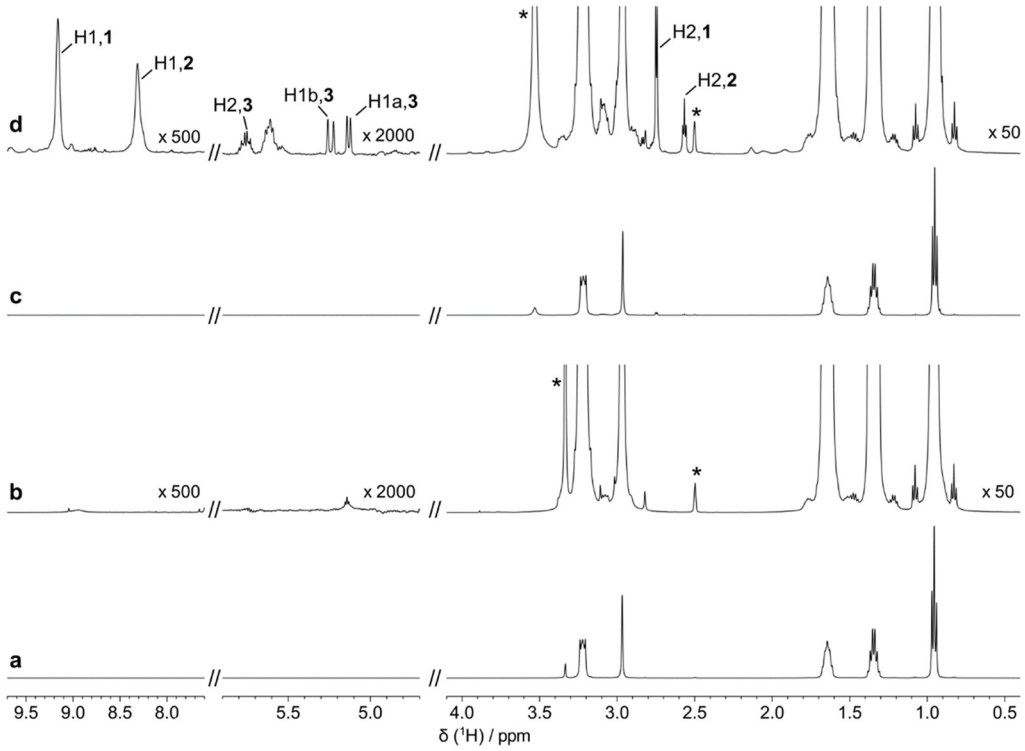

Figure 5. ^{1}H HRMAS NMR spectra of [TBuMA][NTF_2] (**a**,**b**) and 4B168 (**c**,**d**); in (**b**,**d**), the vertical scale used in (**a**,**c**) is expanded by the factors reported on each spectral region. Selected signals of the degradation compounds are labeled as "Hi,j", with i representing the atom number and j indicating the degradation product (Scheme 1). Signals of water protons and residual protons of deuterated DMSO are marked with asterisks.

The dominant thermal degradation products are N-dibutyl-N-methylammonium (1) and N-butyl-N-methylammonium (2), as outlined in Scheme 1; these compounds are compatible with the Hoffman elimination of one or two alkyl chains from the original cation [23]. For these compounds, the signals due to the hydrogen atoms labeled as H1 and H2 in Scheme 1 are clearly observable. Additional signals, characterized by lower

intensities, were assigned to 1-butene (Scheme 1, compound 3), in agreement with the hypothesized degradation pathway. These assignments are indicated in Figure 5, where the signals are labeled as "Hi,j", with i representing the atom number and j the degradation product. The amount of compounds 1 and 2 was determined from the ^{1}H spectra of all the samples, with respect to the amount of the original cation B, using the integrals of the H2,1 and H2,2 signals. Figure 6 shows the values of these integrals as a function of the heating time, where the intensity of the corresponding signal of the non-degraded ionic liquid, occurring at 2.97 ppm, is arbitrarily set to 100. It was, thus, found that, even at the longest heating time, about six molecules of compound 1 and two molecules of compound 2 were present every 100 molecules of ionic liquid cation. This estimate agrees with that obtained using H1,1 and H1,2 signals. Interestingly, the concentration of compound 2 increased at a slower rate than compound 1, in agreement with the fact that the formation of compound 2 requires the preliminary formation of compound 1. Moreover, the amount of compound 3 was always much lower than that expected on the basis of the stoichiometry of the degradation pathways, as clearly evident from the large scaling factor necessary to visualize the signals of this compound (Figure 5d). This can be explained by the volatility of 1-butene or its further degradation/reactions. The presence of 1-butene is compatible with the alkene absorption band between 3200 and 3100 cm^{-1} detected by FTIR (3090 cm^{-1} in the FTIR spectrum of butene in the vapor gas phase). Unfortunately, the absence of specific absorption lines prevented the detection of compounds 1 and 2 in the FTIR spectra.

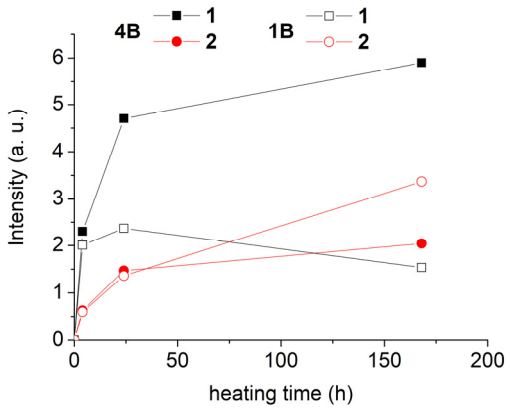

Figure 6. Intensity of H2,1 (black squares) and H2,2 (red circles) signals as a function of the heating time, as obtained from the ^{1}H HRMAS NMR spectra of B, 4B4, 4B24 and 4B168 (filled symbols) and of B, 1B4, 1B24 and 1B168 (empty symbols). The intensity value is relative to that of H2 protons of the non-degraded ionic liquid, which was set to 100 in all spectra.

The ^{1}H NMR spectra recorded after heating for up to 168 h in the presence of metal plates do not show significant differences with respect to the 4B168 spectrum (Figure 7). The main signals of the NMR spectrum of 4B168 are those of the original ionic liquid. For both steel and copper, the spectral lines are broadened, with steel inducing larger line broadening of the signals compared to copper. This broadening, not observed in the case of brass, is probably due to the presence of dissolved paramagnetic metal ions resulting from corrosion of the metal/alloy. Figure 8 shows that the signals of the degradation compounds 1, 2 and 3 are also present in the spectra of samples 1B168 and 3B168, whereas, in the case of 2B168, only sharp signals, due to compound 3, are observed. In the latter case, if compounds 1 and 2 are present, their concentration is below detection limits. However, the occurrence of 1-butene signals suggests that the elimination reactions sketched in Scheme 1 also take place in the presence of copper. The absence of the H1,1 and H1,2 signals could be explained by hypothesizing that the ammonium compounds 1 and 2 release H^{+} and the amine formed coordinates to a copper ion. A similar mechanism has been suggested to rationalize the extraction of Cu^{2+} ions from aqueous solutions using protic ammonium

ionic liquids [24]. However, due to the large linewidth of the signals, it was not possible to confirm this hypothesis.

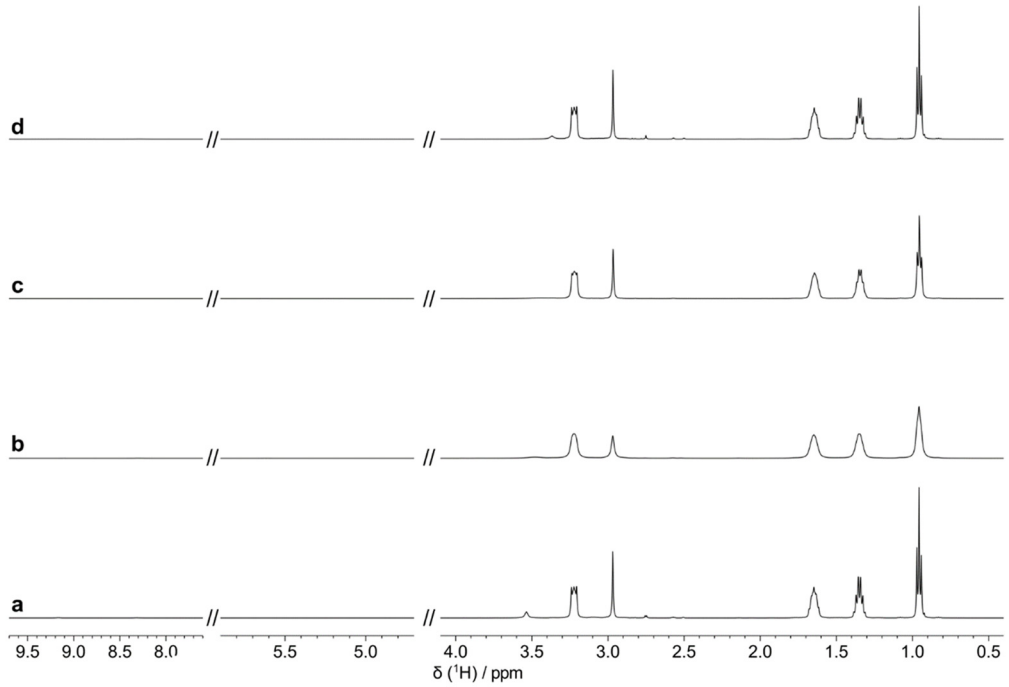

Figure 7. ^{1}H HRMAS NMR spectra of 4B168 (**a**), 1B168 (**b**), 2B168 (**c**), and 3B168 (**d**).

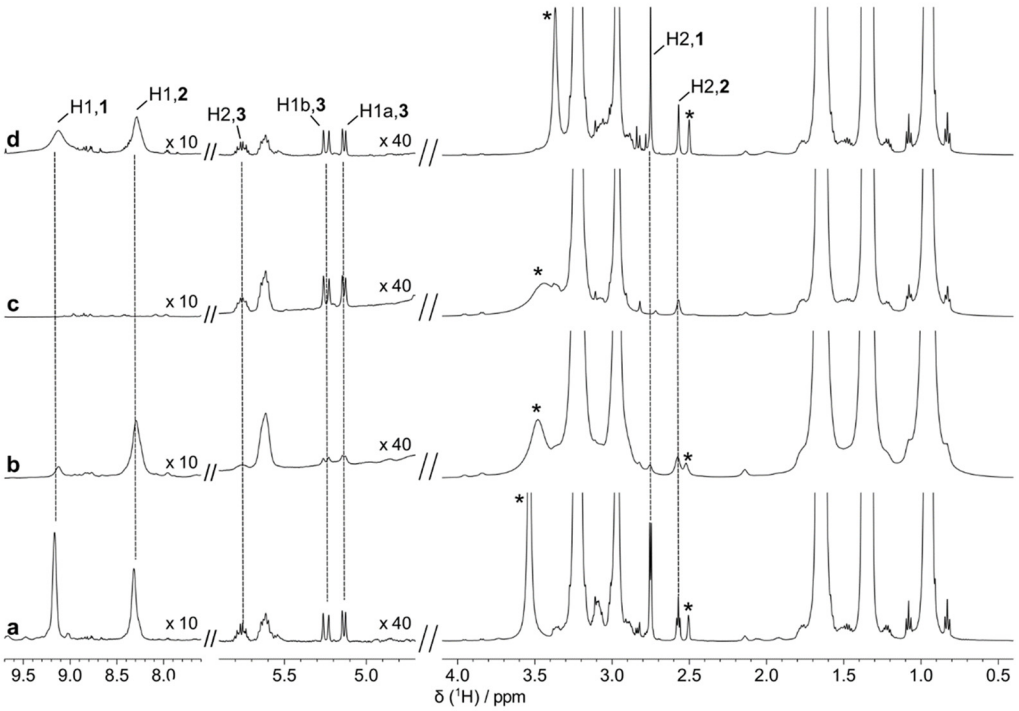

Figure 8. Expansions of ^{1}H HRMAS NMR spectra of 4B168 (**a**), 1B168 (**b**), 2B168 (**c**), and 3B168 (**d**). Expansion factors are reported for each region. Selected signals of the degradation compounds are labeled using the same notation as that applied in Figure 5. Water (3.3–3.6 ppm) and residual DMSO-d_5 (2.50 ppm) signals are marked with asterisks.

For the samples degraded in the presence of steel, the kinetics of formation of compounds 1 and 2 were monitored. Figure 6 shows the trends of the intensity of the H2,1 and

H2,2 signals as a function of heating time in the samples degraded in the presence and absence of metals. The kinetics of formation of compound 2 from compound 1 seems to be accelerated by steel.

HS-GCMS analysis was performed on the 168 h aged samples, with the aim of observing possible volatile degradation compounds in the most extreme condition. Figure 9 shows the peak area of nine main compounds identified in samples B, 4B168, 1B168, 2B168 and 3B168; these are cyclohexane, butanal, ethyl acetate, tert-butanol, methyl-vinyl ketone, N,-N-dimethylformamide, 2-ethyl-1-hexanol and benzothiazole. However, 1-butene was not detected, likely because it was lost in the pre-analytical phase, considering its high volatility, or because of its oxidation. The relevant result is, indeed, the release of butanal in the 3B168 sample, i.e., in the IL treated with copper. We can hypothesize that copper and copper particles may act as catalyzers for the further reaction of butene. Recently, several authors have reported the remarkable long-term stability and high selectivity towards alkenes of Cu nanoparticles as a promising alternative to replace precious-metal-based catalysts in selective hydrogenation [25]. It must be pointed out that even the concentration of butanal was too low to be detected by FTIR and NMR. These volatiles probably result from minor side reactions occurring during the degradation process.

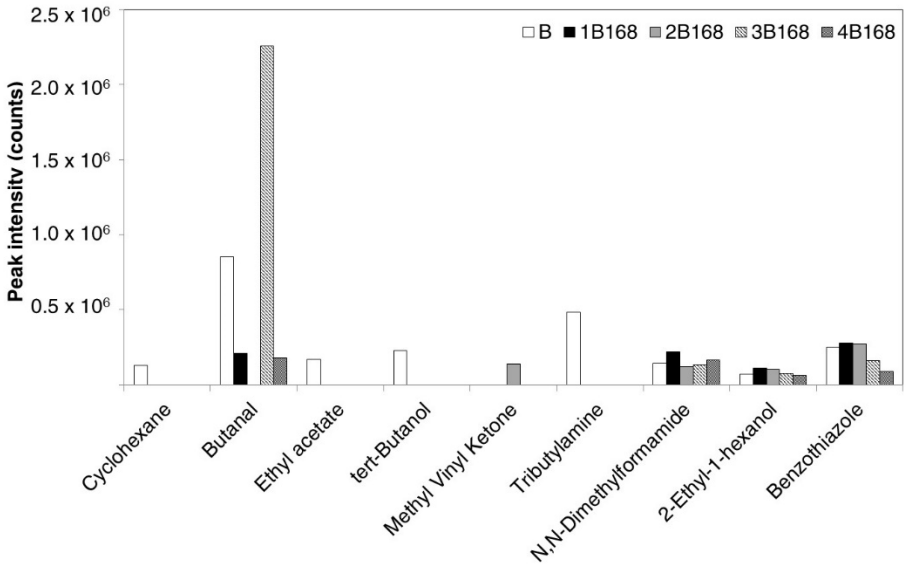

Figure 9. Relative intensity (counts) of 9 main compounds identified in samples B, 4B168, 1B168, 2B168 and 3B168 samples by HS-GCMS analysis.

4. Conclusions

The structural characterization of the ionic liquid [TBuMA][NTF_2], both fresh and after thermal treatment, with or without different metals, was carried out by HRMAS NMR and FTIR spectroscopic analyses, while HS-GC-MS was employed to reveal the formation of volatile compounds. The degradation products of [TBuMA][NTF_2] were characterized after thermal treatment at 200 °C for 4, 24 and 168 h in contact with AISI 304 steel, copper or brass, and without metals as a comparison. The combination of the above-mentioned techniques evidenced the occurrence of degradation processes of the cation. The data suggested a degradation mechanism compatible with the Hoffman elimination of one or two alkyl chains from the cation, with 1-butene being one of the degradation products after thermal treatment, both in the absence or presence of metal plates. The proposed multi-technique approach was revealed to be suitable for the characterization of the degradation compounds of [TBuMA][NTF_2] after thermal treatment in the presence of metals, thus proving to be a promising method for the selection of IL compounds that possess high stability and a suitable lifetime to meet the durability requirements of commercial and industrial solar thermal applications.

Supplementary Materials: The following supporting information can be downloaded at https://www.mdpi.com/article/10.3390/app12031652/s1: Figure S1: comparison of ^{1}H HRMAS spectrum of 4B168 (a,d) with 1D selective ^{1}H TOCSY obtained by irradiating H1,1 (9.16 ppm, b), H1,2 (8.31 ppm, c) and H1a,3 (5.13 ppm, e).; Figure S2: ^{1}H–^{13}C HSQC spectrum of 4B168; Table S1: assignment of ^{1}H and ^{13}C NMR signals of the ionic liquid B; Table S2: assignment of ^{1}H and ^{13}C NMR signals of the degradation compounds 1, 2 and 3.

Author Contributions: Conceptualization, A.F., S.P., E.B. (Emilia Bramanti) and A.L.; methodology, A.F., S.P., E.B. (Emilia Bramanti) and A.L.; investigation, F.N., S.P., E.B. (Emilia Bramanti), B.C., A.L. and E.B. (Enrico Berretti); writing—original draft preparation, A.F., S.P., E.B. (Emilia Bramanti); writing—review and editing, F.N., C.F., A.L., E.B. (Emilia Bramanti), S.P.; supervision, A.F., C.F.; funding acquisition, A.F., A.L. All authors have read and agreed to the published version of the manuscript.

Funding: This research was funded by the FELIX project (Fotonica ed Elettronica Integrate per l'Industria, project code no. 6455) and project MIUR Cluster CTN02_00018 «Energia» Codice progetto CTN02_00018_10016852 "NeMESi".

Conflicts of Interest: The authors declare no conflict of interest.

References

1. Welton, T. Ionic liquids: A brief history. *Biophys. Rev.* **2018**, *10*, 691–706. [CrossRef] [PubMed]
2. Paul, T.C.; Morshed, A.K.M.M.; Fox, E.B.; Visser, A.E.; Bridges, N.J.; Khan, J.A. Thermal performance of ionic liquids for solar thermal applications. *Exp. Therm. Fluid Sci.* **2014**, *59*, 88–95. [CrossRef]
3. Zhang, Z.; Salih, A.A.M.; Li, M.; Yang, B. Synthesis and characterization of functionalized ionic liquids for thermal storage. *Energy Fuels* **2014**, *28*, 2802–2810. [CrossRef]
4. Wadekar, V. V Ionic liquids as heat transfer fluids—An assessment using industrial exchanger geometries. *Appl. Therm. Eng.* **2017**, *111*, 1581–1587. [CrossRef]
5. Das, L.; Rubbi, F.; Habib, K.; Aslfattahi, N.; Saidur, R.; Baran Saha, B.; Algarni, S.; Irshad, K.; Alqahtani, T. State-of-the-art ionic liquid & ionanofluids incorporated with advanced nanomaterials for solar energy applications. *J. Mol. Liq.* **2021**, *336*, 116563.
6. Macfarlane, D.R.; Tachikawa, N.; Forsyth, M.; Pringle, J.M.; Howlett, P.C.; Elliott, G.D.; Davis, J.H.; Watanabe, M.; Simon, P.; Angell, C.A. Energy applications of ionic liquids. *Energy Environ. Sci.* **2014**, *7*, 232–250. [CrossRef]
7. Valkenburg, M.E.V.; Vaughn, R.L.; Williams, M.; Wilkes, J.S. Thermochemistry of ionic liquid heat-transfer fluids. *Thermochim. Acta* **2005**, *425*, 181–188. [CrossRef]
8. Salgado, J.; Parajó, J.J.; Fernández, J.; Villanueva, M. Long-term thermal stability of some 1-butyl-1-methylpyrrolidinium ionic liquids. *J. Chem. Thermodyn.* **2014**, *74*, 51–57. [CrossRef]
9. Monteiro, B.; Maria, L.; Cruz, A.; Carretas, J.M.; Marçalo, J.; Leal, J.P. Thermal stability and specific heats of coordinating ionic liquids. *Thermochim. Acta* **2020**, *684*, 178482. [CrossRef]
10. Liu, J.; Wang, F.; Zhang, L.; Fang, X.; Zhang, Z. Thermodynamic properties and thermal stability of ionic liquid-based nanofluids containing graphene as advanced heat transfer fluids for medium-to-high-temperature applications. *Renew. Energy* **2014**, *63*, 519–523. [CrossRef]
11. Huddleston, J.G.; Visser, A.E.; Reichert, W.M.; Willauer, H.D.; Broker, G.A.; Rogers, R.D. Characterization and comparison of hydrophilic and hydrophobic room temperature ionic liquids incorporating the imidazolium cation. *Green Chem.* **2001**, *3*, 156–164. [CrossRef]
12. Huang, Y.; Chen, Z.; Crosthwaite, J.M.; Aki, S.N.V.K.; Brennecke, J.F. Thermal stability of ionic liquids in nitrogen and air environments. *J. Chem. Thermodyn.* **2021**, *161*, 106560. [CrossRef]
13. Kosmulski, M.; Gustafsson, J.; Rosenholm, J.B. Thermal stability of low temperature ionic liquids revisited. *Thermochim. Acta* **2004**, *412*, 47–53. [CrossRef]
14. Maton, C.; De Vos, N.; Stevens, C.V. Ionic liquid thermal stabilities: Decomposition mechanisms and analysis tools. *Chem. Soc. Rev.* **2013**, *42*, 5963–5977. [CrossRef] [PubMed]
15. Perissi, I.; Bardi, U.; Caporali, S.; Fossati, A.; Lavacchi, A.; Vizza, F. Ionic liquids: Electrochemical investigation on corrosion activity of ethyl-dimethyl-propylammonium bis(trifluoromethylsulfonyl)imide at high temperature. *Russ. J. Electrochem.* **2012**, *48*, 434–441. [CrossRef]
16. Perissi, I.; Bardi, U.; Caporali, S.; Fossati, A.; Lavacchi, A. Ionic liquids as diathermic fluids for solar trough collectors' technology: A corrosion study. *Sol. Energy Mater. Sol. Cells* **2008**, *92*, 510–517. [CrossRef]
17. Verma, C.; Ebenso, E.E.; Quraishi, M.A.; Hussain, C.M. Recent developments in sustainable corrosion inhibitors: Design, performance and industrial scale applications. *Mater. Adv.* **2021**, *2*, 3806–3850. [CrossRef]
18. Perissi, I.; Bardi, U.; Caporali, S.; Lavacchi, A. High temperature corrosion properties of ionic liquids. *Corros. Sci.* **2006**, *48*, 2349–2362. [CrossRef]

19. Pisarova, L.; Gabler, C.; Dörr, N.; Pittenauer, E.; Allmaier, G. Thermo-oxidative stability and corrosion properties of ammonium based ionic liquids. *Tribol. Int.* **2012**, *46*, 73–83. [CrossRef]
20. Cao, Y.; Mu, T. Comprehensive Investigation on the Thermal Stability of 66 Ionic Liquids by Thermogravimetric Analysis. *Ind. Eng. Chem. Res.* **2014**, *53*, 8651–8664. [CrossRef]
21. Alam, M.T.; Jenkins, E.J. HR-MAS NMR Spectroscopy in Material Science. In *Advanced Aspects of Spectroscopy*; Farrukh, M.A., Ed.; IntechOpen: London, UK, 2012; pp. 279–306.
22. Ilharco, L.M.; Garcia, A.R.; Hargreaves, E.C.; Chesters, M.A. Comparative reflection-absorption infrared spectroscopy study of the thermal decomposition of 1-hexene on Ru(0001) and on Pt(111). *Surf. Sci.* **2000**, *459*, 115–123. [CrossRef]
23. Sowmiah, S.; Srinivasadesikan, V.; Tseng, M.C.; Chu, Y.H. On the chemical stabilities of ionic liquids. *Molecules* **2009**, *14*, 3780–3813. [CrossRef] [PubMed]
24. Janssen, C.H.C.; Macías-Ruvalcaba, N.A.; Aguilar-Martínez, M.; Kobrak, M.N. Copper extraction using protic ionic liquids: Evidence of the Hofmeister effect. *Sep. Purif. Technol.* **2016**, *168*, 275–283. [CrossRef]
25. Totarella, G.; Beerthuis, R.; Masoud, N.; Louis, C.; Delannoy, L.; De Jongh, P.E. Supported Cu Nanoparticles as Selective and Stable Catalysts for the Gas Phase Hydrogenation of 1,3-Butadiene in Alkene-Rich Feeds. *J. Phys. Chem. C* **2021**, *125*, 366–375. [CrossRef] [PubMed]